MODELING COMPLEX CELLS IN V1 OF ALERT MONKEYS

Igor Kagan[1], Moshe Gur[2], Max Snodderly[3]

[1] Caltech, Pasadena, CA; [2] Technion, Haifa, Israel; [3] Medical College of Georgia, Augusta, GA

VISION RESEARCH LAB

Supported by NIH EY12243

1. INTRODUCTION

There is a renewed interest in definition, characterization and function of V1 simple and complex cells. The source of input to complex cells and organization of their receptive fields is a subject of ongoing debate. All extant models, feed-forward and recurrent, explain well-documented (in *anaesthetized* cats and monkeys) nonlinear features of complex cells such as sign-of-contrast (polarity) and spatial-phase invariance and nonlinear spatial summation. However, many nonlinear neurons in *alert* monkeys show more diverse and elaborate behaviors deviating from traditional notion of complex cells. Prevalence of nonlinear complex cells in monkey V1 underlines their importance in visual processing and necessitates their careful analysis.

The goals of the present (ongoing) study are:
(1) To characterize spatial and temporal properties of complex cells in various conditions.
(2) To evaluate existing models against experimental results.
(3) To develop more realistic models compatible with a wide range of complex cell behaviors.

2. METHODS

2.1 Neurophysiology

Extracellular responses of single V1 neurons were recorded while alert monkeys performed a fixation task. Classical receptive fields (CRF) were mapped with sweeping and flashing bars and edges and classified as *simple* or *complex* based on the spatial overlap of **increment** and **decrement** activating regions (ARs). Least-square Gaussian profiles were fitted to bar response histograms in order to estimate CRF spatial parameters:

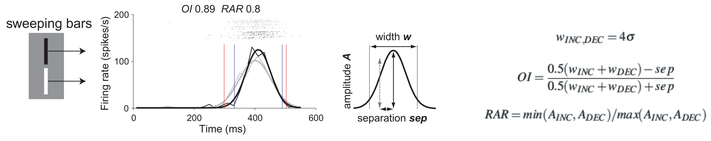

$$w_{INC,DEC} = 4\sigma$$

$$OI = \frac{0.5(w_{INC}+w_{DEC}) - sep}{0.5(w_{INC}+w_{DEC}) + sep}$$

$$RAR = min(A_{INC}, A_{DEC})/max(A_{INC}, A_{DEC})$$

Then neurons were studied with drifting and counterphase (contrast-reversal) gratings of systematically varied spatial frequency (SF), temporal frequency (TF) and patch width (W), optimally oriented and centered on the CRF. Responses were Fourier-analyzed and relative modulation (*RM=F1/F0*, the ratio of 1st and 0th harmonics) was calculated for all stimulus conditions.

2.2 Modeling

The receptive fields (RFs) of model subunits (afferent inputs) are simulated as linear spatiotemporal filters. For simplicity we consider only spatial dimension that is perpendicular to the neuron's preferred orientation. Each subunit is characterized by a spatial RF $\psi(x)$ (Gaussian, DoG or Gabor function) and a temporal impulse response (TIR) $h(t)$. Formally, for Gabor function:

$$\psi(x) = \frac{1}{\sqrt{2\pi}\sigma} exp\left[-\frac{x^2}{2\sigma^2}\right] cos(2\pi\rho x + \phi) \quad (1)$$

where ρ is the tuning spatial frequency, σ is the space constant, and ϕ is the spatial phase.

The subunit's TIR is described by a difference between $(m+1)-$ and $(n+1)-$ stage lowpass filters:

$$h(t) = H(t)\left[\gamma\frac{\alpha(\alpha t)^m exp[-\alpha t]}{m!} - \delta\frac{\beta(\beta t)^n exp[-\beta t]}{n!}\right] \quad (2)$$

where H is Heaviside's unit step function and all parameters are positive. The TIR is monophasic when δ=0, and monophasic, biphasic or triphasic otherwise. TIR in temporal quadrature is obtained by convolving a given TIR with $q(t) = -1/(\pi t)$ (Hilbert transform).

Visual stimuli are presented as spatiotemporal functions $S(x,t)$. For each subunit i we first perform integration over space:

$$g_i(t) = \int_{-\infty}^{\infty} S(x,t)\psi(x)dx \quad (3)$$

and then we convolve the resulting function $g_i(t)$ with a subunit's TIR $h_i(t)$:

$$V_i(t) = h_i(t) * g_i(t) \quad (4)$$

Then subunits are half-wave rectified and summed, and the resulting model response V_m represents an idealization of extracellular firing rate:

$$V_m(t) = \sum_{i=1}^{n} [V_i(t)] \quad (5)$$

All simulations are performed using custom software written in MATLAB.

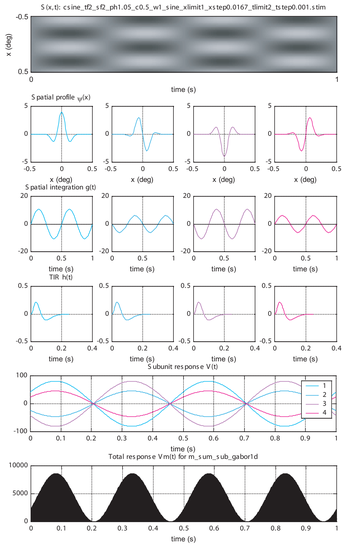

3. RESULTS

3.1 Spatial organization of V1 receptive fields

Most complex cells have strongly overlapping and ~ balanced increment and decrement ARs:

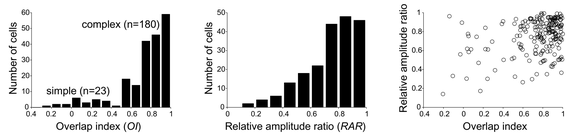

3.2 Relative modulation and spatial (im)balance

Still, many complex cells exhibit strong *F1* modulation to drifting gratings. We tested whether incomplete spatial overlap or amplitude difference between increment and decrement ARs could account for *F1* responses of complex cell, in the model that sums rectified responses of two ARs. For similar ranges of *OI*s and *RAR*s, the correlation between *RM* and overall spatial (im)balance (*I=OI·RAR*) is much weaker and corresponding levels of RM much higher in the data than in the model ($r_{complex}$ = -0.17, r_{model} = -0.88). Thus, high *F1* cannot be fully explained by a static spatial imbalance of increment and decrement ARs.

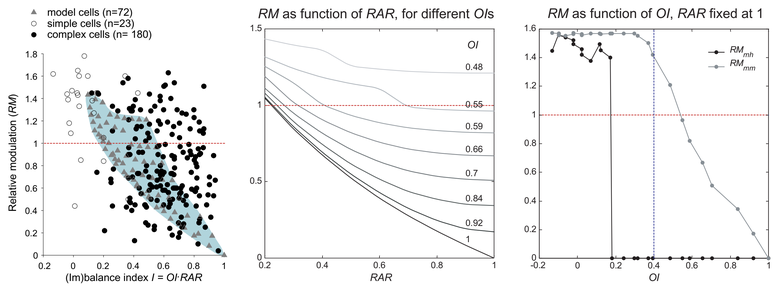

3.3 Modulation patterns depend on stimulus parameters

While complex cells show a variety of responses both within a cell and across cells, several principle systematic patterns are discernible:
1) Drifting gratings of very low spatial frequency cause frequency-doubling (*F2*).
2) Drifting gratings of low-to-mid spatial frequency cause pseudo-linear *F1* modulation.
3) Further increase of spatial frequency removes *F1* harmonic and yields *F0* or "sub*F1*" firing.
4) Low drift temporal frequency (1-2 Hz) tends to evoke *F2* or mixed (*F1-F2-F3*) response, while higher (4-5 Hz) temporal frequency yields *F1* harmonic.
5) Increase of grating patch width often cancels *F2* harmonic and increases *RM*.
6) Responses to counterphase gratings are typically frequency-doubled; deviations from a typical *F2* response: low spatial frequency and/or high temporal frequency transforms even-harmonic to *F1* modulation, similarly to drifting case.

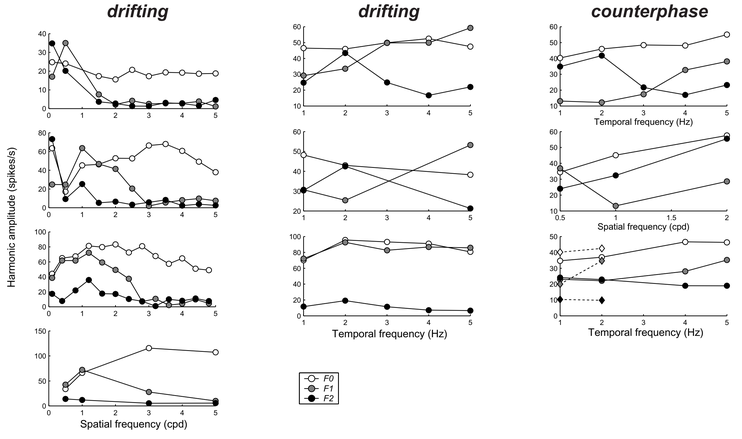

3.4 Shortcomings of energy models

Clearly, the energy model cannot generate F1 responses to drifting gratings. Moreover, when we unbalance increment and decrement components by perturbing location or amplitude of input subunits, the resulting dependence of modulation on grating spatial frequency does not follow experimental trends described in 3.3, except for frequency-doubling at very low *SF*. Similar results were obtained using models that sum multiple even-Gabor subunit pairs.

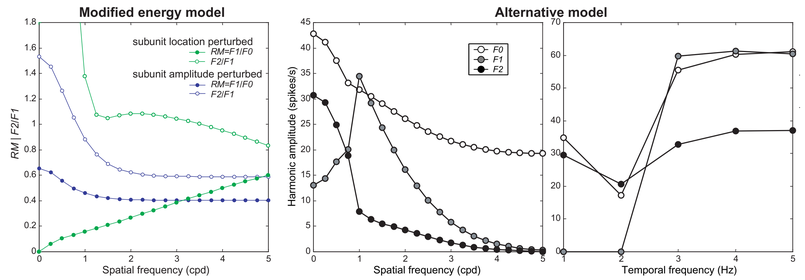

3.5 Alternative model: separate increment and decrement channels, mutual suppression

- No "push-pull" mode.
- Perfectly balanced increment / decrement channels.
- Each channel contains transient and sustained subunits.
- Mutual inhibition between channels with fixed time constant of 100 ms.
- When two polarities are present in the input, only one (first) channel is firing.

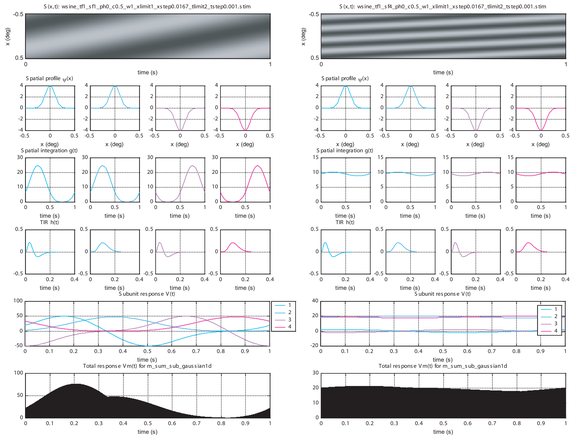

4. SUMMARY

4.1 Conclusions

Complex cells exhibit behaviors incompatible with current models, particularly variants of the energy model.

Static spatial imbalance of increment and decrement ARs is not strong enough to yield observed levels of F1 modulation, and cannot account for dependence of the harmonic content on stimulus spatial and temporal frequency.

We could not find a simple amendment to any of existing models that would render it compatible with complex mutually-inconsistent behaviors (which is probably not surprising...). Our results suggests that the timing of suppressive interactions and other temporal effects are crucial, but the exact mechanism has yet to be elucidated. A simple "First-Takes-All" model was able to reproduce effects of spatial and temporal frequency consistent with data.

4.2 Future work

1) Incorporate effects of overlapping surrounds.

2) Incorporate recurrent connections and synaptic depression.

3) Cell-by-cell parameter estimation and comparison of data with model performance.

References, Appendix, code and additional info: igor@vis.caltech.edu

http://igoresha.virtualave.net/Work/Cosyne04